European Polymer Journal 101 (2018) 202–210

Contents lists available at ScienceDirect

European Polymer Journal

journal homepage: www.elsevier.com/locate/europolj

Size control of cross-linked carboxy-functionalized polystyrene particles: Four orders of magnitude of dimensional versatility

Nina M. Sekerak[a], Kristin M. Hutchins[a,b], Binbin Luo[c,d], Jin Gu Kang[c,d], Paul V. Braun[c,d,b], Qian Chen[c,d,a], Jeffrey S. Moore[a,b,d,*]

[a] Department of Chemistry, University of Illinois at Urbana-Champaign, Urbana, IL 61801, United States
[b] The Beckman Institute for Advanced Science and Technology, University of Illinois at Urbana-Champaign, Urbana, IL 61801, United States
[c] Department of Materials Science and Engineering, University of Illinois at Urbana-Champaign, Urbana, IL 61801, United States
[d] Frederick Seitz Materials Research Laboratory, University of Illinois at Urbana-Champaign, Urbana, IL 61801, United States

ARTICLE INFO

Keywords:
Particle synthesis
Size control
Morphology
Functionalization
Cross-linking density
Swelling

ABSTRACT

Synthesis of functionalized organic particles is an expanding area of exploration due to versatile potential applications including imaging agents, drug delivery vehicles, and supported synthesis. A robust, customizable method that allows modification of size, degree of cross–linking, identity of the crosslinker, and desired functionality, while retaining particle integrity would be highly advantageous. Here, we report the straightforward, versatile syntheses of cross-linked carboxy polystyrene (PS) particles ranging from 50 nm to 500 µm in diameter that retain their morphology in organic solvents. Removal of a protecting group exposed free benzoic acid groups that were readily functionalized to afford peroxide, ester, or amide moieties. The identity and density of the crosslinker were also systematically modified to alter the swelling properties of the microparticles. The particles were rigorously characterized by IR and ^{13}C NMR spectroscopy, SEM, and optical imaging. The methods reported here provide a robust and reliable way to systematically and reproducibly synthesize functionalized cross-linked PS-based particles spanning a wide range of sizes.

1. Introduction

The synthesis of polystyrene (PS) particles with size control is of significant interest due to their numerous applications [1,2]. Small (e.g., 10–700 nm diameter), monodisperse PS particles find applications as biomedical imaging agents [3], catalytic scaffolds [4], building blocks for photonic crystals [5], drug delivery agents [6], and binders for paints and coatings [7]. On the other hand, polydisperse PS resins that are tens of microns or more in diameter are also useful and serve as solid-state supports for reagents [8,9] and catalysts [10], as well as packing materials for ion-exchange columns [11]. A variety of attached functional groups including hydroxyl, alkyl, amino, and thiol moieties have been incorporated into these particles [12–17], which enables their use in such broad and numerous applications.

Although particle synthesis has been an area of research exploration for nearly a century, reliable methods that achieve control over size and functionality remain challenging. Many organic nanoparticles (< 1 µm diameter) lose their morphology when suspended in organic solvents, and particle morphology varies significantly depending on the synthetic method. Changing internal and external reaction parameters such as concentration, stir rate, and reaction vessel design significantly alters the resulting particle size and morphology [18]. In this regard, reported methods for synthesizing polymeric particles are not always reproducible based on provided procedures. Also, developments in microscopy technology now enable thorough imaging characterization, often missing from classical and even some contemporary publications. Synthesizing particles with control over size, functionality, and cross-linking density is advantageous for systematic studies that vary particle characteristics [19,20]. Furthermore, the ability to attach a variety of functional groups is desirable for tuning particle chemistry for specific applications [21,22]. Carboxylic acid groups are amenable to a variety of coupling techniques; however, maintaining control over size and functionality while incorporating acid moieties into PS particles and during subsequent synthetic modification is a persistent challenge [23,34]. For example, Okada et al., recently demonstrated synthesis of hydroxyapatite ($Ca_{10}(PO_4)_6(OH)_2$) nanoparticle-coated PS microspheres utilizing PS with carboxyl end groups (carboxy-PS), which interact with the calcium ion of hydroxyapatite during emulsion. The carboxy-PS spheres underwent dramatic reductions in volume (ca. 99%) following the emulsion, and low molecular weight spheres experienced significant deformation [23]. Landfester et al., reported the preparation of carboxyl- and amino-functionalized

* Corresponding author at: The Beckman Institute for Advanced Science and Technology, University of Illinois at Urbana-Champaign, Urbana, IL 61801, United States.
E-mail address: jsmoore@illinois.edu (J.S. Moore).

https://doi.org/10.1016/j.eurpolymj.2018.01.028
Received 22 November 2017; Received in revised form 4 January 2018; Accepted 26 January 2018
Available online 31 January 2018
0014-3057/

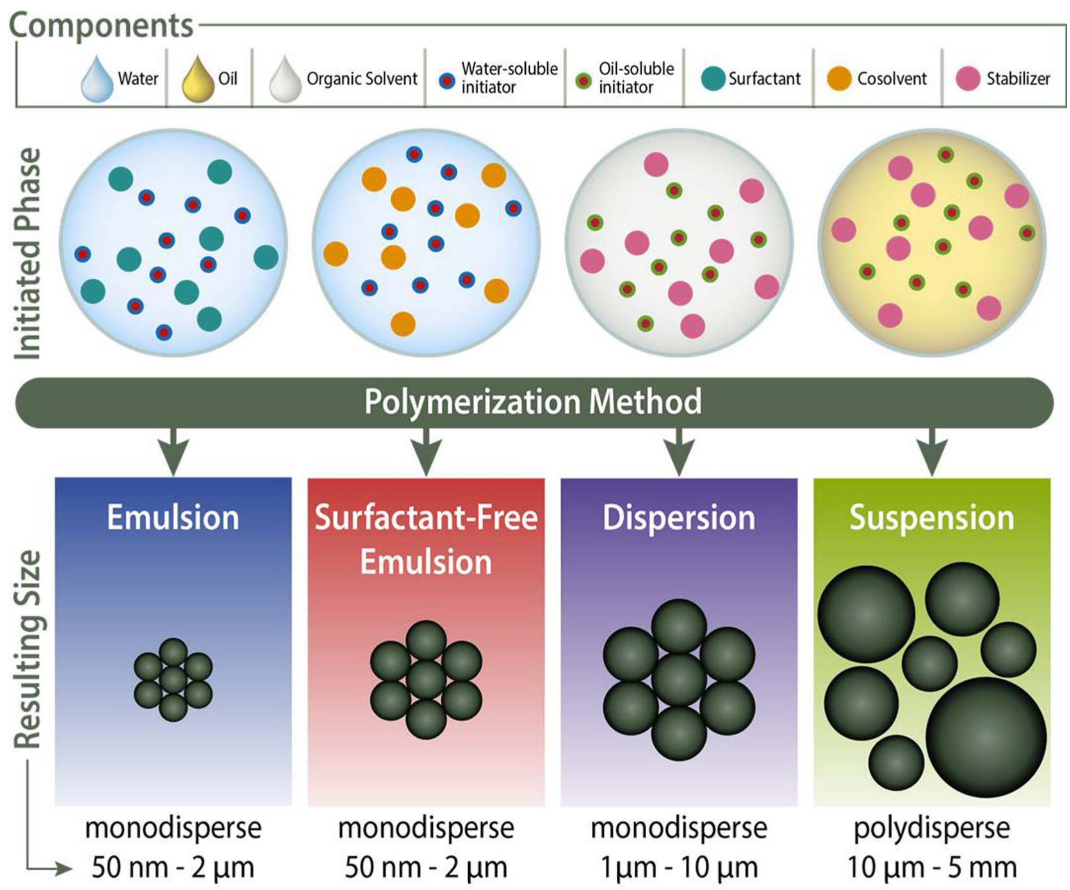

Scheme 1. Methods for the synthesis of cross-linked PS particles spanning a range of sizes.

PS particles via miniemulsion polymerization; however, bimodal size distributions were observed and latexes synthesized using ionic surfactants were not resistant to electrolytes [30]. Jamshaid et al., recently described the synthesis of magnetic carboxyl-functionalized particles ranging from ca. 275–500 nm in size. An oil-in-water magnetic seeded emulsion technique was used, followed by a second emulsion polymerization with methacrylic acid to increase the amount of carboxylic acid groups [35].

While carboxy-PS resins and nanoparticle solutions are available commercially [36], customized variations in the degree of cross--linking, identity of the crosslinker, and desired functionality are somewhat limited. To address these challenges, we systematically tuned the polymerization method and reliably synthesized cross-linked carboxy-PS particles with size control to access particles spanning four orders of magnitude in diameter (Scheme 1). The polymerization methods comprise emulsion, surfactant-free emulsion, dispersion, and suspension polymerization, which collectively provide a series of functionalized particles of varying sizes. The incorporation of a cross-linker allows the particles to be manipulated in organic solvents while retaining morphology. Usage of an acid-protected comonomer (*tert*-butyl-4-vinylbenzoate) afforded robust particles that can be functionalized to esters, amides, and peroxides following removal of the protecting group post polymerization. Finally, the degree of cross-linking and cross-linker moiety was varied to afford microparticles that exhibit differences in their ability to swell in organic solvents.

2. Experimental

2.1. Materials

The 500 mL three-neck flasks and stirrer bearing were purchased from Chemglass Life Sciences (24/40 joints, item numbers: CG-1524-05 (flask) and CG-2071 (stirrer bearing)). The 300 mL three-neck flasks and glass stirrer shaft were purchased from Wilmad-LabGlass (24/40 joints, product numbers: LG-7331-184 (flask) and LG-9500-100 (stirrer)). The Teflon stir blades were purchased from VWR (catalog number: 89062064). A Glas-Col GT Series mechanical stirring system (catalog number: 099D GT31, 333 rpm end was used) and an IKA digital mechanical stirrer (model number: RN20 D2M.n S1) were used for the polymerization reactions. Unless otherwise stated, all reagents were obtained from commercial suppliers and used without further purification. Water was obtained from a Millipore (Billerica, MA) Milli-Q water purification system. The inhibitors were removed by passage through basic alumina. The *tert*-butyl 4-vinylbenzoate comonomer (**1**) was prepared as reported (see Supplementary Information (SI)) [37,38].

2.2. Synthesis of nanoparticles below 100 nm in diameter via emulsion polymerization (2A)

In a 500-mL three-neck flask, water (250 mL), sodium dodecyl sulfate (SDS, 0.35 g, 1.2 mmol), potassium persulfate (KPS, 0.775 g, 2.87 mmol), styrene (19.0 g, 182 mmol), and divinylbenzene (DVB, 0.96 g, 7.4 mmol) were stirred at ca. 180 rpm by a Glas-Col GT Series mechanical stirrer (motor speed set to 60%). The flask was purged with nitrogen for 15 min and then heated to 70 °C. After 1 h, a mixture of **1** (2.3 g, 11 mmol) and DVB (0.21 g, 1.6 mmol) was added to the reaction mixture by syringe, and the mixture was heated for an additional 12 h. After cooling to room temperature, the particles were isolated by centrifugation at 6000 rpm for 15 min. The particles were redispersed in tetrahydrofuran (THF, 15 mL), precipitated by addition of ethanol (EtOH, 35 mL), and centrifuged at 6000 rpm for 15 min. This process was repeated an additional four times. The particles were dried *in vacuo* to give a white solid (18.2 g, 82% yield).

2.3. Synthesis of nanoparticles ca. 600 nm in diameter via surfactant-free emulsion polymerization (2B)

In a 500-mL three-neck flask, water (144 mL), methanol (MeOH, 18.0 g, 22.8 mL), KPS (0.225 g, 0.83 mmol), and styrene (16.1 g, 155 mmol) were stirred at ca. 180 rpm by a Glas-Col GT Series mechanical stirrer (motor speed set to 60%). The flask was purged with nitrogen for 15 min and then heated to 70 °C. After 1 h, a mixture of **1** (2.0 g, 9.8 mmol) and DVB (0.20 g, 1.5 mmol) was added to the reaction mixture by syringe, and the mixture was heated for an additional 12 h. After cooling to room temperature, the particles were isolated by centrifugation at 6000 rpm for 10 min. The particles were redispersed in THF (15 mL), precipitated by addition of EtOH (35 mL), and centrifuged at 6000 rpm for 10 min. This process was repeated an additional four times. The particles were dried *in vacuo* to give a white solid (10.8 g, 59% yield).

To increase particle size, the same experimental procedure as above was conducted; however, the amount of KPS was increased to 1 mmol. The average particle size was slightly larger [30,39] at 650 nm in diameter.

2.4. Synthesis of 1.4 µm mushroom caps via dispersion polymerization (2C)

In a 300-mL three-neck flask, water (3.4 mL), EtOH (64.9 g, 82.2 mL), poly(vinylpyrrolidinone) (PVP, MW ~ 360 kDa, 0.54 g), Triton X-305 solution (0.58 g), azobisisobutyronitrile (AIBN, 0.41 g, 2.5 mmol), and styrene (12.0 g, 115.2 mmol) were stirred at ca. 230 rpm by a Glas-Col GT Series mechanical stirrer (motor speed set to 70%). The flask was purged with nitrogen for 15 min and then heated to 70 °C. After 1 h, a mixture of **1** (1.4 g, 6.9 mmol) and DVB (0.24 g, 1.8 mmol) in EtOH (30.0 g, 38.0 mL) and water (1.58 mL) was purged with nitrogen, heated to 70 °C, and added to the reaction mixture by cannula over a period of 1 h. When the second stage was added over shorter periods of time, mixtures of spherical, di-colloid, and mushroom cap-shaped particles were produced (Fig. S11). The mixture was heated for an additional 12 h. After cooling to room temperature, the particles were isolated by centrifugation at 6000 rpm for 10 min. The particles were redispersed in THF (10 mL), precipitated by addition of EtOH (30 mL) and *n*-hexanes (10 mL), and centrifuged at 6000 rpm for 10 min. The particles were redispersed in THF (10 mL), precipitated by addition of EtOH (40 mL), and centrifuged at 6000 rpm for 10 min. The latter process was repeated an additional three times. The particles were dried *in vacuo* to give a white solid (6.91 g, 51% yield).

2.5. Synthesis of microparticles 10 to 100 µm in diameter via suspension polymerization (2D)

In a 300-mL three-neck flask, water (110 mL), Mowiol 40–88 (PVA, MW ~205,000 g/mol, 88% hydrolyzation, 1.10 g), styrene (16.1 g, 155 mmol), DVB (0.18 g, 1.4 mmol), **1** (2.0 g, 9.8 mmol), and benzoyl peroxide (BPO, Luperox, 0.50 g, 2.1 mmol) were stirred at 400 rpm by an IKA 20 digital mechanical stirrer, purged with nitrogen for 15 min, and heated to 70 °C for 12 h. The particles were isolated by centrifugation at 3000 rpm for three min. The particles were swollen in THF (30 mL), shrunk by addition of EtOH (70 mL), and centrifuged at 3000 rpm for three min. This process was repeated an additional four times. The particles were dried *in vacuo* to give a white solid (13.6 g, 75% yield).

2.6. Synthesis of microparticles 50 to 500 µm in diameter via suspension polymerization (2D)

In a 300-mL three-neck flask, water (110 mL), Mowiol 40–88 (PVA, MW ~ 205,000 g/mol, 88% hydrolyzation, 0.25 g), styrene (16.1 g, 155 mmol), DVB (0.20 g, 1.5 mmol), **1** (2.0 g, 9.8 mmol), and BPO (Luperox, 0.50 g, 2.1 mmol) were stirred at 240 rpm by an IKA 20 digital mechanical stirrer, purged with nitrogen for 15 min, and heated to 70 °C for 12 h. The particles were isolated by centrifugation at 3000 rpm for three min. The particles were swollen in THF (30 mL), shrunk by addition of EtOH (70 mL), and centrifuged at 3000 rpm for three min. This process was repeated an additional four times. The particles were dried *in vacuo* to give a white solid (17.1 g, 94% yield).

2.7. Cleavage of tert-butyl esters (3)

At room temperature (rt), particles of **2** (5.65 g) were suspended in 1:1 dichloromethane (DCM)/trifluoroacetic acid (TFA) (100 mL, *v/v*) and stirred for 12 h. DCM and TFA were removed *in vacuo*. The carboxy-PS particles were washed five times in THF/EtOH by redispersion and centrifugation (the same conditions as the respective protected particles), and dried *in vacuo* to give solid white particles (4.3 g, 80% yield).

2.8. Synthesis of 1-pyrenebutanol functionalized particles (4)

Carboxy-PS **3** (0.30 g, ~0.17 mmol acid) was dispersed in 3.5 mL DCM. To this dispersion, 1-pyrenebutanol (**7**, 0.20 g, 0.73 mmol) and 4-dimethylaminopyridine (DMAP, 0.10 g, 0.80 mmol) were added, followed by *N,N′*-diisopropylcarbodiimide (DIC, 0.03 mL, 0.3 mmol). The mixture was stirred at rt. After 24 h, EtOH (10 mL) was added to the reaction mixture. The particles were isolated by centrifugation (the same conditions as the respective protected particles), washed five times in THF/EtOH by redispersion and centrifugation, and dried *in vacuo* to give white solid particles (0.20 g, 59% yield).

2.9. Synthesis of n-butylamine functionalized particles (5)

Carboxy-PS **3** (0.31 g, ~0.17 mmol acid) was swollen in a solution of 1,1′-carbonyldiimidazole (CDI, 0.13 g, 0.80 mmol) in THF (8 mL) at rt. After 1 h, *n*-butylamine (0.08 mL, 0.81 mmol) in THF (2 mL) was added to the reaction mixture. After another hour, EtOH (10 mL) was added to the reaction mixture. The particles were isolated by centrifugation (the same conditions as the respective protected particles), washed five times in THF/EtOH by redispersion and centrifugation, and dried *in vacuo* to give white solid particles (0.15 g, 49% yield).

2.10. Synthesis of m-chloroperbenzoic acid functionalized particles (6)

Carboxy-PS **3** (1.1 g, ~0.61 mmol acid) was swollen in a solution of *m*-chloroperbenzoic acid (*m*CPBA, 0.98 g, 5.7 mmol) in DCM (25 mL). DIC (0.55 mL, 3.6 mmol) was added, and the mixture was stirred at rt. After 12 h, EtOH (25 mL) was added to the reaction mixture. The particles were isolated by centrifugation (the same conditions as the respective protected particles), washed five times in THF/EtOH by redispersion and centrifugation, and dried *in vacuo* to give white solid particles (1.1 g, 96% yield).

3. Results and discussion

3.1. General approach

The most straightforward and ideal approach involves using a monomer that is readily copolymerized with styrene and modified post-polymerization to yield a carboxylic acid, giving carboxy-PS particles (**3**) (Scheme 2). Two reports have described the synthesis of carboxy-PS nanoparticles utilizing 4-vinylbenzoic acid as a comonomer with styrene; however, to our knowledge, these procedures have not been reproduced in the literature to date [40,41]. The crystallinity and hydrophilicity of 4-vinylbenzoic acid, as well as its limited solubility in styrene, do not suit its use in a biphasic polymerization. To bypass the use of 4-vinylbenzoic acid directly, the acid was masked with a *tert*-butyl ester to yield a hydrophobic oil that is fully miscible with styrene. The *tert*-butyl 4-vinylbenzoate comonomer (**1**) was synthesized via a

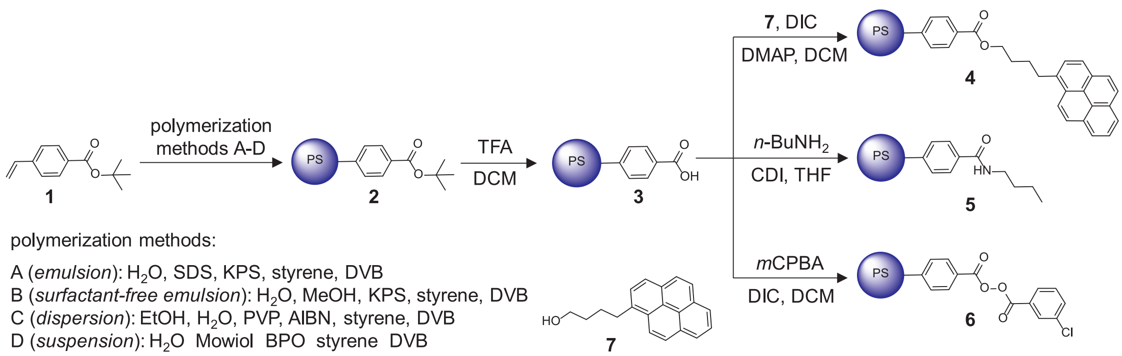

Scheme 2. Synthesis of functionalized polystyrene (PS) particles.

modified literature procedure (see SI) [37]. Following copolymerization with styrene and a crosslinker, the *tert*-butyl group is easily and quantitatively removed under acidic conditions to yield carboxylic acid **3**. This approach successfully enables a route to PS particles functionalized with benzoic acid groups.

3.2. Size control

Monomer **1** was copolymerized with styrene and DVB as a crosslinker in emulsion, surfactant-free emulsion, dispersion, and suspension polymerizations to give protected carboxy-PS particles (**2**) in a variety of sizes (Table 1).

The emulsion polymerization [42] procedure of Zukoski and coworkers was modified to obtain the smallest set of particles [43]. Simultaneous addition of all reagents at the beginning of the procedure produced particles with low cross-linking densities that lost their morphology in organic solvents. Thus, the polymerization was conducted in two stages. First, styrene and a portion of DVB were copolymerized in a solution of SDS and ionic initiator for 1 h, allowing seed particles to form *in situ*. Comonomer **1** was not added in the first stage as it had been observed to widen the polydispersity of the seed particles. Instead, the comonomer **1** and a second portion of DVB were added to the reaction mixture in a second stage following the formation of the seed particles. After 12 h of polymerization, the particles were washed with ethanol (EtOH) and tetrahydrofuran (THF) to remove surfactant and any remaining monomer. The mole percent of the DVB crosslinker was relatively high (4.4 mol%) for nanoparticles; however, at lower cross-linking densities, the particles did not withstand the washing and ester cleavage conditions. The two-stage emulsion polymerization yielded particles of **2** that were approximately 50 nm in diameter before ester cleavage as measured by scanning electron microscopy (SEM) (Fig. 1a).

To obtain particles an order of magnitude larger in diameter, the surfactant-free emulsion polymerization (SFEP) procedure was modified by Homola and coworkers [44] was modified. When the polymerization was conducted in one stage, the particles were more polydisperse than when the addition of reagents was split between two stages. Thus, as for the traditional emulsion polymerization, styrene was added at the beginning of the reaction in order to produce seed particles *in situ* during the first hour of the polymerization, followed by addition of a mixture of comonomer **1** and DVB. Following 12 h of polymerization, the particles were washed with THF and EtOH to remove unreacted monomers. Monodisperse particles of **2** ca. 600 nm in diameter were successfully obtained by this procedure (Fig. 1a). Effects of low cross-linking densities were similar to those observed for the 50 nm particles, and utilizing 0.9 mol% crosslinker afforded particles that were stable in organic solvents (Supplementary Movie S1). Moreover, increasing the initiator concentration slightly increased the diameter of the particles [30,39]. Monodisperse particles of **2** 650 ± 70 nm in diameter were synthesized by increasing the amount of KPS initiator from 0.83 mmol to 1 mmol (Figs. S9–10, Supplementary Movie S3).

Dispersion polymerization [45] was attempted for the preparation of particles with roughly twice the diameter of the SFEP particles. Winnik and coworkers reported the successful synthesis of PS copolymer spheres when the comonomer was added after the nucleation stage [46,47], similar to our emulsion polymerization procedures. Thus, comonomer **1** and the DVB crosslinker were added 1 h following the polymerization onset to allow for the formation of PS seed particles *in situ*. However, dimpling was observed for these particles, resulting in monodisperse mushroom cap-shaped particles of **2** that were ca 1.4 μm in diameter ("brim-to-brim") and 1.0 μm in height ("crown-to-brim") (Fig. 1a,c). This phenomenon has been reported in seeded emulsion polymerizations when solvent or monomer is expelled from a swollen particle faster than solvent is entering a cross-linked particle [48–51]. The time at which the second stage comonomers were added was varied, but other non-spherical morphologies were observed (Fig. S12). The mushroom cap particles can be subjected to ester cleavage conditions, and the mushroom cap shape is generally retained (Fig. 1b).

Suspension polymerization [52] yields polydisperse samples because monomer droplet size determines particle size in the biphasic reaction. Suspension polymerizations are also sensitive to a variety of parameters such as the concentration and type of surfactant or stabilizer used. To obtain larger cross-linked microparticles, several procedures were attempted and altered [53–57]. Many of the reported procedures lacked information such as reaction vessel design, stir rate, and molecular weight of the steric stabilizer, which can affect the size distribution and morphology of the resulting particles. Several stabilizers—such as methyl cellulose, ethylene maleic anhydride copolymer, Brij 58, fluoropolymer, lignosulfonic acid, and PVA of varying molecular weight and degree of hydrolyzation—were tested along with varying stir rates. Our tests of various surfactants agreed with the findings of Puig and coworkers who found that PVA with high molecular weight and 88% hydrolyzation has good stabilization properties for suspension polymerizations [58]. The PVA stabilizer for the reported procedure has a molecular weight of 205,000 g/mol. For a 1.0 wt% aqueous solution

Table 1
Synthetic conditions for preparation of protected carboxy-PS particles of various sizes.

Particle diameter	50 nm	600 nm	50 μm	400 μm
Milli-Q water (mL)	250	144	110	110
Surfactant, cosolvent, or stabilizer (g)	0.35 SDS	18.0 MeOH	1.1 PVA	0.25 PVA
Initiator (g)	0.78 KPS	0.23 KPS	0.50 BPO	0.50 BPO
Styrene (g)	19.0	16.1	16.1	16.1
1, initial (g)	–	–	2.0	2.0
DVB, initial (g)	0.96	–	0.18	0.2
1, after 1 h (g)	2.3	2.0	–	–
DVB, after 1 h (g)	0.21	0.2	–	–
Stir rate (rpm)	180	180	400	240

Abbreviations: DVB (divinylbenzene), SDS (sodium dodecyl sulfate), KPS (potassium persulfate), MeOH (methanol), PVA (poly(vinyl alcohol)), BPO (benzoyl peroxide).

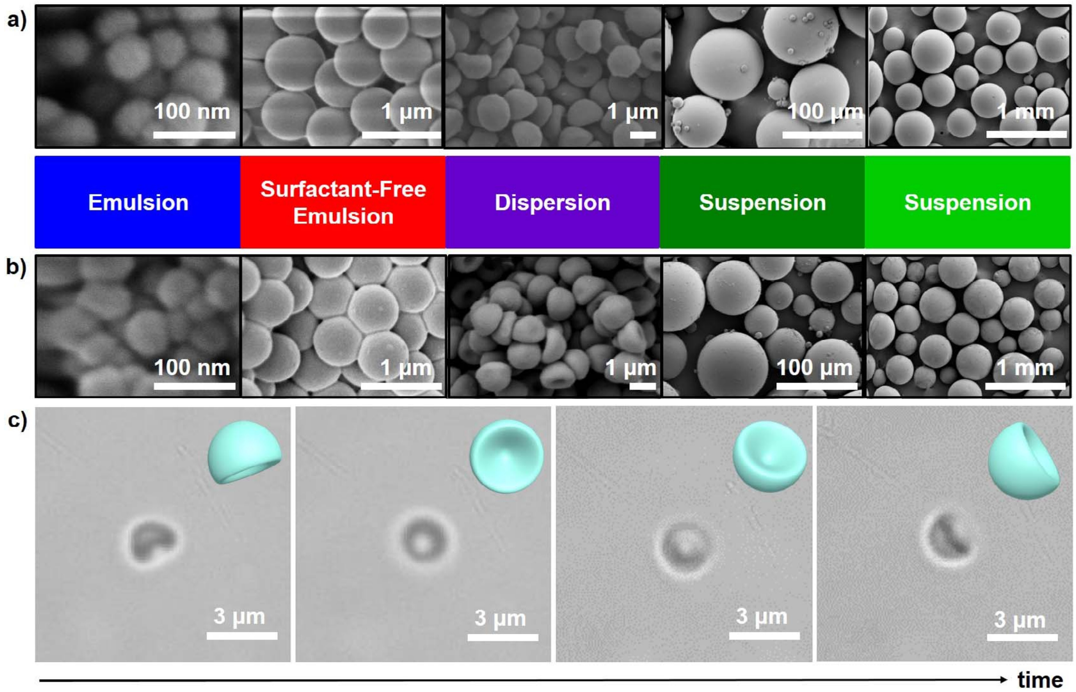

Fig. 1. SEM images of particles (a) **2** and (b) **3**. Polymerization method denoted. Suspension method with 100 µm scale bars utilized 1.0 wt% PVA and 1 mm scale bars utilized 0.23 wt% PVA. (c) Optical microscopy images and schematics showing the rotational dynamics of a mushroom cap-shaped particle of **2** dispersed in a DMF/EtOH solvent mixture (see Supplementary Movie S6).

of PVA and a stir rate of 400 rpm, suspension polymerization yielded spherical particles of **2**, mostly 10–100 µm in diameter. For a 0.23 wt% aqueous solution of PVA and a stir rate of 240 rpm, suspension polymerization afforded larger particles of **2**, mostly 80–500 µm in diameter (Fig. 1a).

3.3. Functionalization and characterization

Following the synthesis of **2** via radical polymerization, the *tert*-butyl ester was cleaved to afford **3** in a variety of sizes with free carboxylic acid groups. Particles of **2** were stirred in a 1:1 (*v*/*v*) mixture of DCM and TFA overnight. Although some discoloration (from white to light yellow) and dimpling were observed for a few samples following ester cleavage, especially those with low degrees of cross-linking, the particles generally retained their shapes and sizes within error (Fig. 1b, Table 2).

The shape and behavior of particles **2** and **3** in organic solvents were studied and recorded by optical microscopy with video imaging. Particles synthesized via SFEP, dispersion polymerization, and suspension polymerization techniques were examined. The particles were dispersed in a DMF/EtOH solvent mixture (volume ratio of 3:1) by sonicating for a period of 30 min, and movies were recorded in real time (see Supplementary Movies S1–S9 and Fig. S14). The movies demonstrate that all particles are easily dispersed in organic solvents and retain morphology once dispersed.

Table 2
Sizes of particles **2** and **3** (before and after ester cleavage) measured by SEM. For each set of particles, 50 particles were measured and averaged. For the mushroom caps, both the diameter (brim-to-brim) and the height (crown to brim) were measured.

Polymerization method	Size of particle **2**	Size of particle **3**
Emulsion	50 ± 10 nm	50 ± 10 nm
SFEP	600 ± 50 nm	620 ± 50 nm
Dispersion (diameter)	1.4 ± 0.1 µm	1.27 ± 0.06 µm
Dispersion (height)	1.0 ± 0.1 µm	0.94 ± 0.09 µm
Suspension (1.0 wt% PVA)	90 ± 30 µm	70 ± 30 µm
Suspension (0.22 wt% PVA)	360 ± 80 µm	360 ± 60 µm

Supplementary Movie S1.

Supplementary Movie S2.

Supplementary Movie S3.

Supplementary Movie S4.

Supplementary Movie S5.

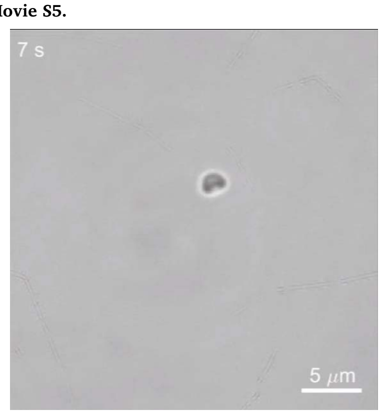

Supplementary Movie S6.

Supplementary Movie S7.

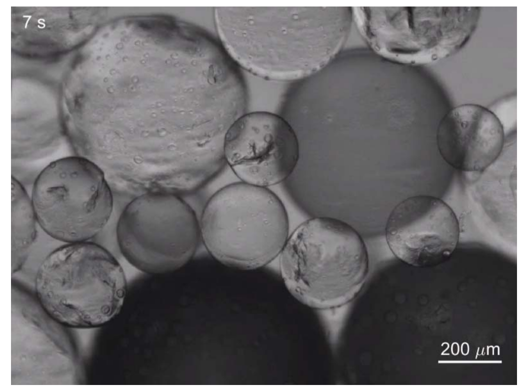

Supplementary Movie S8.

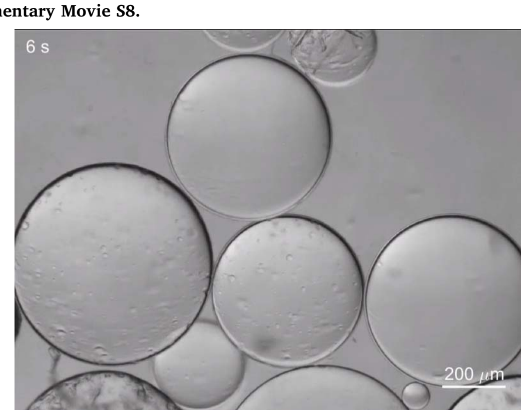

Supplementary Movie S9.

Crystallization of the colloids was attempted by dispersing particles of **3** (650 ± 70 nm, synthesized by SFEP, see SI) in methanol. Numerous solvents were used to disperse the particles, but significant swelling occurred with all solvents, while less swelling occurred in methanol. The particles were allowed to self-assemble overnight at 39 °C. SEM imaging demonstrated that the particles assembled into monolayers, as well as layers composed of two, three, and more than five particles in height (Figs. S15–16). Fourier transform infrared (FTIR) reflectance spectra were collected for the monolayer and multi-layer samples; however, no Bragg reflection was observed between 1.6 and 1.8 μm, indicating that crystallization did not occur (Fig. S17). Dynamic light scattering (DLS) measurements indicated that the polydispersity was too large to achieve crystallization (PDI of ca. 0.07–0.1 (± 40–55 nm) is needed) (Fig. S18).

The chemical functionality of the particles was characterized by FTIR spectroscopy, both by attenuated total reflectance (ATR) and diffuse reflectance (DRIFTS) techniques, as well as by gel-phase ^{13}C NMR spectroscopy. Results obtained from both techniques confirmed

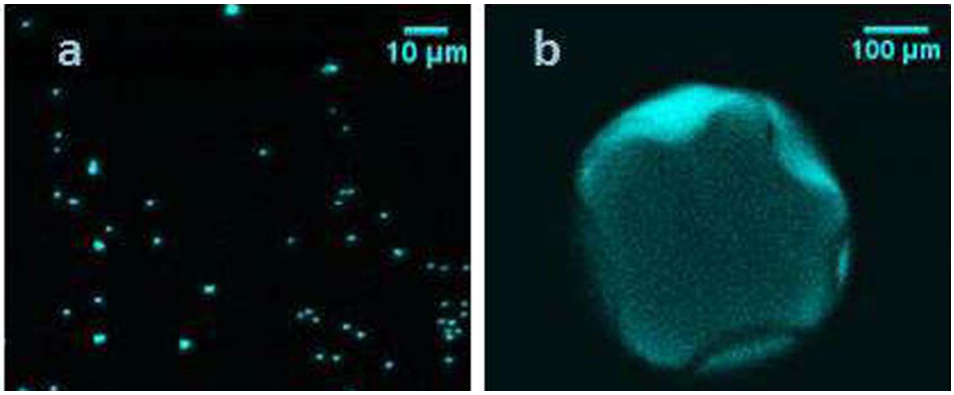

Fig. 2. Confocal microscopy images of fluorescently-labeled **4**: (a) 600 nm particles and (b) a 400 μm particle.

the change in functionality between particles **2** and **3**. In the FTIR spectra, ester **2** showed one sharp carbonyl stretch at 1710 cm^{-1}, a methyl umbrella at 1367 cm^{-1}, and a C—O—C ester stretch at 1290 cm^{-1}, while acid **3** showed two carbonyl stretches at 1740 and 1680 cm^{-1}, corresponding to the free carboxylic acid and the dimerized carboxylic acid (Fig. S5). A residual peak at 1710 cm^{-1} indicated incomplete cleavage for shorter reaction times. Gel-phase ^{13}C NMR spectroscopy before and after removal of the *tert*-butyl group further confirmed cleavage. For ester **2**, signals at 80.4 and 28.3 ppm indicate the presence of the *tert*-butyl group and these peaks are absent in the spectrum of **3**. Following ester cleavage, the carbonyl resonance shifted from 165.7 to 167.5 ppm (Fig. S1). The changes observed in the IR and ^{13}C NMR spectra indicated that full removal of the protecting group was achieved (within limits of detection).

Successful hydrolysis of ester **2** to carboxylic acid **3** enabled further functionalization by coupling techniques. Coupling alcohols, amines and peroxy acids to the carboxylic acid yielded esters, amides, and dibenzoyl peroxides, respectively (Scheme 2). To demonstrate the esterification of the particle-bound carboxylic acid, 1-pyrenebutanol (**7**) was conjugated to **3** via DIC coupling. The resulting particles of **4** were imaged with confocal microscopy and found to be fluorescent (Fig. 2). A control experiment was conducted by repeating the functionalization procedure with **7** in the absence of DIC. These particles did not show fluorescence at the same gain setting. A second control experiment was conducted by subjecting particles of **2** to identical coupling reaction conditions as the particles of **3**, and the resulting particles also did not display fluorescence at the same gain setting. These control experiments indicate that **7** is chemically attached to the particles and not merely adsorbed. Further characterization of **4** by FTIR and NMR spectroscopy demonstrated the formation of an ester bond. In the FTIR spectrum of **4**, the carbonyl stretches of the carboxylic acid were replaced by one sharp peak at 1716 cm^{-1} (Fig. S6). In the ^{13}C NMR spectrum of **4**, the carbonyl peak shifted to 166.6 ppm, while additional aromatic peaks appeared between 122 and 133 ppm. Additional peaks also appeared in the aliphatic region of the spectrum at 29.8, 29.2, 22.4, and 21.0 ppm (Fig. S2).

A different coupling method was used to synthesize an amide derivative and demonstrate synthetic versatility. Coupling via 1,1′-carbonyldiimidazole is an established method [59] that has gained interest in recent decades in the field of peptide synthesis. This coupling technique can also be applied to a variety of products since the reactive acylimidazole intermediate serves as an alternative to an acid chloride. To demonstrate the formation of an amide, the 600-nm and 360-μm particles of **3** were activated with 1,1′-carbonyldiimidazole. Subsequent displacement of the imidazole by a primary amine yielded desired amide **5**. The particles were characterized by gel-phase ^{13}C NMR and FTIR spectroscopy. The ^{13}C NMR spectrum of **5** revealed new peaks corresponding to the alkyl chain at 40.1, 33.1, 21.1, and 14.3 ppm. Additionally, the carbonyl peak shifted from 167.5 to 166.8 ppm (Fig. S3). In the FTIR spectrum of **5**, the carbonyl peaks were replaced by a broad peak at 1658 cm^{-1}, corresponding to the amide (Fig. S7). Both methods indicated a change in the carbonyl region, supportive of the formation of an amide.

Effective functionalization of the particles included not only the formation of ester and amide groups, but also the formation of dibenzoyl peroxides (BPO). Few methods exist to synthesize non-symmetrical peroxides [60–62]. Such peroxides could be utilized as initiator species for synthesizing new material at particle interfaces [38]. Particle **3** was functionalized with BPO by reaction with DIC and *m*CPBA to yield **6**. The particles were characterized by FTIR and gel-phase ^{13}C NMR spectroscopy. In the FTIR spectrum of **6**, the carbonyl stretches of the acid disappeared, while two carbonyl stretches

Table 3
Volume swelling ratios of microparticles of **3** with different crosslinkers and cross-linking densities. The amount of crosslinker is reported in mmol per gram of comonomer (styrene and **1**) mixture. For each value, the swelling of ten particles were measured and averaged.

Crosslinker (mmol/g)	Chemical structure	THF swelling ratio	DCM swelling ratio	Toluene swelling ratio
DVB (0.032)	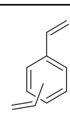	7.1 ± 0.9	4.1 ± 0.4	3.7 ± 0.3
DVB (0.063)		5.1 ± 0.5	4.2 ± 0.4	3.7 ± 0.1
DVB (0.24)		3.7 ± 0.2	3.2 ± 0.2	3.0 ± 0.1
EGDMA (0.033)	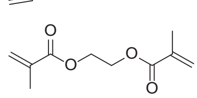	14.1 ± 0.9	5.8 ± 0.8	4.9 ± 0.3
EGDMA (0.063)		8.4 ± 0.9	4.3 ± 0.5	3.9 ± 0.2
EGDMA (0.24)		4.0 ± 0.3	3.2 ± 0.3	3.2 ± 0.1
PEGDMA (0.031)	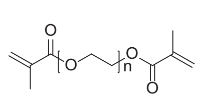	8.2 ± 0.9	4.3 ± 0.2	4.2 ± 0.3
PEGDMA (0.062)		6.1 ± 0.9	3.7 ± 0.3	3.6 ± 0.2
PEGDMA (0.25)		3.9 ± 0.3	2.9 ± 0.3	2.9 ± 0.2

corresponding to the non-symmetric peroxide appeared at 1789 and 1766 cm^{-1} (Fig. S8) [63]. The ^{13}C NMR spectrum of **6** also indicated the disappearance of the carboxylic acid. Two peaks corresponding to the carbonyl groups of the peroxide appeared at 163.2 and 162.5 ppm, while three new peaks in the aromatic region appeared at 135.8, 135.1, and 131.5 ppm (Fig. S4). Since the acid peak was not visible in the FTIR or NMR spectra, it can be assumed that the particles underwent complete functionalization (within limits of detection).

3.4. Cross-linking effects

To demonstrate the versatility of the suspension polymerization method, the cross-linker identity and density were varied. Three different crosslinkers were used: DVB, ethylene glycol dimethacrylate (EGDMA), and poly(ethylene glycol) dimethacrylate (PEGDMA, M_n 550) (Table 3). Crosslinker amounts of approximately 0.35, 0.7, and 2.5 mol% were used (Table S1). Following reaction workup, the particles were swollen in THF, dichloromethane (DCM), or toluene. The diameter of the particle was measured by optical microscopy before and after swelling (Fig. S13). Ten particles of each type were swollen in the noted solvent, and the average swelling ratios are listed in Table 3. The volume swelling ratio is equal to the cube of the swollen particle diameter divided by the cube of the non-swollen particle diameter. Particles showed the largest swelling ratio in THF and the smallest in toluene. Particles with higher percentages of cross-linking displayed lower swelling ratios than those with lower percentages of cross-linking. Particles with DVB as a crosslinker swelled less when compared to particles with the other two crosslinkers. The particles cross-linked with EGDMA had the largest swelling ratios. Thus, both the percentage and identity of the crosslinker affects the swelling ratio.

4. Conclusion

We have demonstrated a straightforward, versatile route to synthesizing carboxy-functionalized PS particles of various and controllable sizes consisting of the copolymerization of a protected acid monomer with styrene and a crosslinker in an emulsion, surfactant-free emulsion, dispersion, or suspension polymerization. This family of procedures enabled production of particles ranging from 50 nm to 500 µm in diameter. Removal of the *tert*-butyl protecting group exposed free benzoic acid groups, which could be coupled with alcohols, amines, and peracids to afford ester-, amide-, and peroxide-functionalized particles. The crosslinker was varied for the microparticles to probe particle swelling capacity. Particles with low percentages of EGDMA crosslinker displayed the highest volume-swelling ratio. The methods reported here provide a toolkit for synthesizing cross-linked particles that lie within a desired size range, retain morphology in organic solvents, and can be further functionalized for a variety of applications.

Author contributions

The manuscript was written through contributions of all authors. All authors have given approval to the final version of the manuscript.

Acknowledgment

This work was supported by the U.S. Department of Energy, Division of Materials Sciences under Award Number DE-FG02-07ER46471, through the Frederick Seitz Materials Research Laboratory at the University of Illinois at Urbana–Champaign.

Appendix A. Supplementary material

Experimental details, NMR and IR spectra, SEM images, optical images, DLS data, movies of particles in organic solvents. The following files are available free of charge. Supporting information, spectra, and images (PDF) Supplementary movies of particles (.avi files). Supplementary data associated with this article can be found, in the online version, at http://dx.doi.org/10.1016/j.eurpolymj.2018.01.028.

References

[1] L.B. Sebrell, Charles goodyear memorial lecture. The second mile, Ind. Eng. Chem. 35 (1943) 736–750.
[2] I. Ostromislensky, Process for Making Powdered Vitreous Polymerized Styrol and its Homologues, to the Powder so Produced, and Articles Including Such Material. U.S. Patent 1,676,281, July 10, 1928.
[3] D. Shi, H.S. Cho, Y. Chen, H. Xu, H. Gu, J. Lian, W. Wang, G. Liu, C. Huth, L. Wang, R.C. Ewing, S. Budko, G.M. Pauletti, Z. Dong, Fluorescent polystyrene–Fe_3O_4 composite nanospheres for in vivo imaging and hyperthermia, Adv. Mater. 21 (2009) 2170–2173.
[4] P.D. Stevens, J. Fan, H.M.R. Gardimalla, M. Yen, Y. Gao, Superparamagnetic nanoparticle-supported catalysis of suzuki cross-coupling reactions, Org. Lett. 7 (2005) 2085–2088.
[5] X. Xu, S.A. Asher, Synthesis and utilization of monodisperse hollow polymeric particles in photonic crystals, J. Am. Chem. Soc. 126 (2004) 7940–7945.
[6] K.S. Soppimath, T.M. Aminabhavi, A.R. Kulkarni, W.E. Rudzinski, biodegradable polymeric nanoparticles as drug delivery devices, J. Control. Release 70 (2001) 1–20.
[7] H.A. Scholz, History of water-thinned paints, Ind. Eng. Chem. 45 (1953) 709–711.
[8] S.V. Ley, I.R. Baxendale, R.N. Bream, P.S. Jackson, A.G. Leach, D.A. Longbottom, M. Nesi, J.S. Scott, R.I. Storer, S.J. Taylor, Multi-step organic synthesis using solid-supported reagents and scavengers: a new paradigm in chemical library generation, J. Chem. Soc., Perkin Trans. 1 (2000) 3815–4195.
[9] P.H.H. Hermkens, H.C.J. Ottenheijm, D. Rees, Solid-phase organic reactions: a review of the recent literature, Tetrahedron 52 (1996) 4527–4554.
[10] C.A. McNamara, M.J. Dixon, M. Bradley, Recoverable catalysts and reagents using recyclable polystyrene-based supports, Chem. Rev. 102 (2002) 3275–3300.
[11] J.S. Fritz, Factors affecting selectivity in ion chromatography, J. Chromatogr. A 1085 (2005) 8–17.
[12] D.R. Breed, R. Thibault, F. Xie, Q. Wang, C.J. Hawker, D.J. Pine, Functionalization of polymer microspheres using click chemistry, Langmuir 25 (2009) 4370–4376.
[13] O. Lunov, T. Syrovets, C. Loos, G.U. Nienhaus, V. Mailänder, K. Landfester, M. Rouis, T. Simmet, Amino-functionalized polystyrene nanoparticles activate the NLRP3 inflammasome in human macrophages, ACS Nano 5 (2011) 9648–9657.
[14] A. Búcsi, J. Forcada, S. Gibanel, V. Héroguez, M. Fontanille, Y. Gnanou, Monodisperse polystyrene latex particles functionalized by the macromonomer technique, Macromolecules 31 (1998) 2087–2097.
[15] J.M.J. Fréchet, M.D. de Smet, M.J. Farrall, Functionalization of crosslinked polystyrene resins: 2. Preparation of nucleophilic resins containing hydroxyl or thiol functionalities, Polymer 20 (1979) 675–680.
[16] B.R. Stranix, J.P. Gao, R. Barghi, J. Salha, G.D. Darling, Functional polymers from (vinyl)polystyrene. short routes to binding functional groups to polystyrene resin through a dimethylene spacer: bromine, sulfur, phosphorus, silicon, hydrogen, boron, and oxygen, J. Org. Chem. 62 (1997) 8987–8993.
[17] G.D. Darling, J.M.J. Fréchet, Chemical modification of polystyrene resins. Approaches to the binding of reactive functionalities to polystyrene resins through a two-carbon spacer, J. Org. Chem. 51 (1986) 2270–2276.
[18] S. Kawaguchi, M.A. Winnik, K. Ito, Dispersion copolymerization of n-butyl methacrylate with poly(ethylene oxide) macromonomers in methanol-water. Comparison of experiment with theory, Macromolecules 28 (1995) 1159–1166.
[19] M.T. Gokmen, F.E. Du Prez, Porous polymer particles-A comprehensive guide to synthesis, characterization, functionalization and applications, Prog. Polym. Sci. 37 (2012) 365–405.
[20] Y. Chen, P. Espeel, S. Reinicke, F.E.D. Prez, M.H. Stenzel, Control of glycopolymer nanoparticle morphology by a one-pot, double modification procedure using thiolactones, Macromol. Rapid. Commun. 35 (2014) 1128–1134.
[21] R.F.A. Teixeira, O. van den Berg, L.-T.T. Nguyen, K. Fehér, F.E. Du Prez, Microencapsulation of active ingredients using PDMS as shell material, Macromolecules 47 (2014) 8231–8237.
[22] T. Dispinar, C.A.L. Colard, F.E. Du Prez, Polyurea microcapsules with a photocleavable shell: UV-triggered release, Polym. Chem. 4 (2013) 763–772.
[23] M. Okada, H. Maeda, S. Fujii, Y. Nakamura, T. Furuzono, Formation of pickering emulsions stabilized via interaction between nanoparticles dispersed in aqueous phase and polymer end groups dissolved in oil phase, Langmuir 28 (2012) 9405–9412.
[24] C.R. Harrison, P. Hodge, J. Kemp, G.M. Perry, Introduction of carboxyl groups into crosslinked polystyrene, Makromol. Chem. 176 (1975) 267–274.
[25] A.R. Vaino, K.D. Janda, Solid-phase organic synthesis: a critical understanding of the resin, J. Comb. Chem. 2 (2000) 579–596.
[26] N. Marti, F. Quattrini, A. Butté, M. Morbidelli, Production of polymeric materials with controlled pore structure: the “reactive gelation” process, Macromol. Mater. Eng. 290 (2005) 221–229.
[27] A.Y. Men'shikova, Y.O. Skurkis, T.G. Evseeva, Z.P. Shkarubskaya, T.B. Tennikova, S.S. Ivanchev, Binding of protein to polystyrene particles in the presence of polyvinylpyrrolidone in the surface layer, Russ. J. Appl. Chem 77 (2004) 2011–2016.
[28] S.D. Kim, E.M. Boczar, A. Klein, L.H. Sperling, Effect of surface segregation of ionic end groups on polystyrene latex early-time interdiffusion, Langmuir 16 (2000) 1279–1284.

[29] S.N. Song, W. Zhang, Z.Q. Hu, Z.C. Zhang, Monodisperse micrometer-size carboxyl-functionalized polystyrene particles obtained by two-stage radiation-induced dispersion polymerization, Colloids Surf. APhysicochem. Eng. Aspects 348 (2009) 1–8.

[30] A. Musyanovych, R. Rossmanith, C. Tontsch, K. Landfester, Effect of hydrophilic comonomer and surfactant type on the colloidal stability and size distribution of carboxyl- and amino-functionalized polystyrene particles prepared by miniemulsion polymerization, Langmuir 23 (2007) 5367–5376.

[31] T. Itoh, T. Tamamitsu, H. Shimomoto, E. Ihara, Surface structure and composition of narrowly-distributed functional polystyrene particles prepared by dispersion polymerization with poly(l-glutamic acid) macromonomer as stabilizer, Polymer 70 (2015) 183–193.

[32] J. Choi, S.Y. Kwak, S. Kang, S.S. Lee, M. Park, S. Lim, J. Kim, C.R. Choe, S.I. Hong, Synthesis of highly crosslinked monodisperse polymer particles: effect of reaction parameters on the size and size distribution, J. Polym. Sci., Part A: Polym. Chem. 40 (2002) 4368–4377.

[33] M.J. Farrall, J.M.J. Fréchet, Bromination and lithiation: two important steps in the functionalization of polystyrene resins, J. Org. Chem. 41 (1976) 3877–3882.

[34] M. Nishiya, T. Sugimoto, M. Kobayashi, Electrophoretic mobility of carboxyl latex particles in the mixed solution of 1:1 and 2:1 electrolytes or 1:1 and 3:1 electrolytes: experiments and modeling, Colloids Surf. APhysicochem. Eng. Aspects 504 (2016) 219–227.

[35] T. Jamshaid, M.M. Eissa, Q. Lelong, A. Bonhommé, G. Augsti, N. Zine, A. Errachid, A. Elaissari, Tailoring of carboxyl-decorated magnetic latex particles using seeded emulsion polymerization, Polym. Adv. Technol. 28 (2017) 1088–1096.

[36] For example, see Sigma-Aldrich, Spherotech, and Magsphere Inc.

[37] A.B. Smith, C.A. Risatti, O. Atasoylu, C.S. Bennett, J. Liu, H. Cheng, K. TenDyke, Q. Xu, Design, synthesis, and biological evaluation of diminutive forms of (+)-spongistatin 1: lessons learned, J. Am. Chem. Soc. 133 (2011) 14042–14053.

[38] K.M. Hutchins, N.M. Sekerak, J.S. Moore, Polymerization initiated by particle contact: a quiescent state trigger for materials synthesis, J. Am. Chem. Soc. 138 (2016) 12336–12339.

[39] J.R. Leiza, E.D. Sudol, M.S. El-Aasser, Preparation of high solids content poly(n-butyl acrylate) latexes through miniemulsion polymerization, J. Appl. Polym. Sci. 64 (1997) 1797–1809.

[40] R.A. Prasath, K. Margarit-Puri, M. Klapper, Emulsifier-free emulsion polymerization of styrene with 4-vinylbenzoic acid: kinetics and distribution of the carboxyl groups, J. Appl. Polym. Sci. 103 (2007) 2910–2919.

[41] A. Mantel, N. Barashkov, I. Irgibayeva, A. Kiriy, V. Senkovskyy, In Free-Radical Quaternary Copolymerisation of Styrene, 4-Vinylbenzoic acid, 9-Vinylanthracene and 2-Vinylnaphthalene: Composition of Prepared Copolymers, Polymer Preprints, American Chemical Society, Division of Polymer Chemistry, 2012, pp. 189–190.

[42] A.R. Goodall, M.C. Wilkinson, J. Hearn, Mechanism of emulsion polymerization of styrene in soap-free systems, J. Polym. Sci., Polym. Chem. Ed. 15 (1977) 2193–2218.

[43] E.B. Mock, H. De Bruyn, B.S. Hawkett, R.G. Gilbert, C.F. Zukoski, Synthesis of anisotropic nanoparticles by seeded emulsion polymerization, Langmuir 22 (2006) 4037–4043.

[44] A.M. Homola, M. Inoue, A.A. Robertson, Experiments with soap-free polymerization of styrene in the presence of alcohols, J. Appl. Polym. Sci. 19 (1975) 3077–3086.

[45] K.P. Lok, C.K. Ober, Particle-size control in dispersion polymerization of polystyrene, Can. J. Chem. 63 (1985) 209–216.

[46] J.-S. Song, M.A. Winnik, Cross-linked, monodisperse, micron-sized polystyrene particles by two-stage dispersion polymerization, Macromolecules 38 (2005) 8300–8307.

[47] J.-S. Song, L. Chagal, M.A. Winnik, Monodisperse micrometer-size carboxyl-functionalized polystyrene particles obtained by two-stage dispersion polymerization, Macromolecules 39 (2006) 5729–5737.

[48] M. Okubo, H. Minami, Production of micron-sized monodispersed anomalous polymer particles having red blood corpuscle shape, Macromol. Symp. 150 (2000) 201–210.

[49] L. Xu, H. Li, X. Jiang, J. Wang, L. Li, Y. Song, L. Jiang, Synthesis of amphiphilic mushroom cap-shaped colloidal particles towards fabrication of anisotropic colloidal crystals, Macromol. Rapid Commun. 31 (2010) 1422–1426.

[50] A. Srisopa, A.M.I. Ali, A.G. Mayes, Understanding and preventing the formation of deformed polymer particles during synthesis by a seeded polymerization method, J. Polym. Sci., Part A: Polym. Chem. 49 (2011) 2070–2080.

[51] E.Y.K. Fung, K. Muangnapoh, C.M. Liddell Watson, Anisotropic photonic crystal building blocks: colloids tuned from mushroom-caps to dimers, J. Mater. Chem. 22 (2012) 10507–10513.

[52] E. Vivaldo-Lima, P.E. Wood, A.E. Hamielec, A. Penlidis, An updated review on suspension polymerization, Ind. Eng. Chem. Res. 36 (1997) 939–965.

[53] D.A. Davis, A. Hamilton, J. Yang, L.D. Cremar, D. Van Gough, S.L. Potisek, M.T. Ong, P.V. Braun, T.J. Martinez, S.R. White, J.S. Moore, N.R. Sottos, Force-induced activation of covalent bonds in mechanoresponsive polymeric materials, Nature 459 (2009) 68–72.

[54] S. Durie, K. Jerabek, C. Mason, D.C. Sherrington, One-pot synthesis of branched poly(styrene-divinylbenzene) suspension polymerized resins, Macromolecules 35 (2002) 9665–9672.

[55] P.H. Toy, T.S. Reger, P. Garibay, J.C. Garno, J.A. Malikayil, G.-Y. Liu, K.D. Janda, Polytetrahydrofuran cross-linked polystyrene resins for solid-phase organic synthesis, J. Comb. Chem. 3 (2001) 117–124.

[56] J.A. Greig, D.C. Sherrington, Electrophilic substitution of highly crosslinked polystyrene resins, Eur. Polym. J. 15 (1979) 867–871.

[57] L.R. Melby, D.R. Strobach, Oligonucleotide syntheses on insoluble polymer supports. I. Stepwise synthesis of trithymidine diphosphate, J. Am. Chem. Soc. 89 (1967) 450–453.

[58] E. Mendizabal, J.R. Castellanos-Ortega, J.E. Puig, A method for selecting a polyvinyl alcohol as stabilizer in suspension polymerization, Colloids Surf. 63 (1992) 209–217.

[59] H.A. Staab, M. Lüking, F.H. Dürr, The preparation of imidazolides. synthesis of amides, hydrazides, and hydroxamic acids by the imidazolide method, Chem. Ber. 95 (1962) 1275–1283.

[60] J.I.G. Cadogan, 570. Reactions of pyridyl benzoates with some perbenzoic acids, J. Chem. Soc. (1959) 2844–2846.

[61] C.G. Swain, W.H. Stockmayer, J.T. Clarke, Effect of structure on the rate of spontaneous thermal decomposition of substituted benzoyl peroxides, J. Am. Chem. Soc. 72 (1950) 5426–5434.

[62] R.J. Linhardt, B.L. Murr, E. Montgomery, J. Osby, J. Sherbine, Mechanism for diacyl peroxide decomposition, J. Org. Chem. 47 (1982) 2242–2251.

[63] F.D. Greene, J. Kazan, Preparation of diacyl peroxides with N,N′-dicyclohexylcarbodiimide, J. Org. Chem. 28 (1963) 2168–2171.